Local Driving Assistance from Demonstration for Mobility Aids

James Poon[1], Yunduan Cui[2], Jaime Valls Miro[1], Takamitsu Matsubara[2] and Kenji Sugimoto[2]

***Abstract*— Active assistive mobility systems are largely limited to *a-priori* mapped environments, whereas their reactive assistive counterparts are in general location independent and focus on the provision of collision avoidance in the immediate space surrounding the platform. This paper presents a framework capable of providing active short-term navigation, combining the intelligence of active assistance with the freedom of location independence. Demonstration data from an able expert while driving the mobility aid in a standard indoor setting is used off-line to learn reference behavioral models of navigation given perceptual information from the platform surroundings and the input controls exerted by the user while navigating. These serve as the foundation for on-line probabilistic short-term destination inference using the instantaneously available data from the user and on-board sensors. This is coupled with a real-time stochastic optimal path generation able to exploit the same short term demonstration paths from the expert with the belief they capture both the driver's awareness of the platform's physical geometry and appropriate behaviors for their surroundings. Experimental results with users of varying proficiency in a setting unvisited in training data show promise in using the framework in assisting users experiencing difficulty in safe power mobility aid use.**

I. Introduction

The global population is ageing quickly, with predictions that the worldwide proportion of people aged 60 and over is expected to nearly double by 2050 [1]. Mobility assistance aids for the elderly and frail promote independence and self-esteem in their users, and as such there is a strong motivation within the research community to develop intelligent systems capable of providing advanced mobility assistance to these populations [2]. The anticipated benefit of these advances to alleviate the substantial time devoted by carers on everyday mobility supervision, that could be otherwise spent on supplementary aspects of care, also appears compelling. Our objective is to thus develop an aid framework that can be incorporated into power mobility devices (PMDs) - such as the one shown in Fig. 1 - fit to be continuously used without undue resistance or dependance on the part of the user to support them during navigational activity. Since PMDs are large, heavy and powerful machines there are strict conditions an applicant must meet before prescription is approved [3] even if they are otherwise capable of independenly performing other routine tasks. In this light, the target end users of this work are those who retain some independence but can benefit from assistance in mobility to avoid potential damage to themselves or their surroundings, rather than individuals requiring constant oversight due to more complex healthcare or lifestyle requirements.

Fig. 1: UTS semi-autonomous wheelchair.

The fundamental proposition of this work is to learn both short-term "local" intention estimation and their associated confined planning strategies from data acquired from sensors mounted on the platform without reliance upon objectives drawn from static locations, so that the proposed intelligent PMD can extrapolate these learnings to new places and different users. This is done through models built from an able 'expert' driving the PMD around a known and mapped environment while position, joystick input and sensor data, in our case a planar laser scanner, are logged. For intention estimation a behavioral model is built allowing for a discrete distribution of likelihoods across points in a moving window around the PMD, to be inferred only upon immediately available sensor information and user input (generally taken to be 2D joystick measurements). Here we define intention as likely points in the local surroundings of the PMD that the user may reasonably wish to stop at or pass through at a given instant. The procedure for obtaining this model from training expert data is described in Section II.

We also propose a methodology to facilitate the learning of short-term path planning and user compliance from the same training data set in Section III. Short local paths are decomposed into primitives which are spatially scalable to desired intentions. As this does not ensure safety, we combine these paths with sensor data and refine them via a stochastic optimal control method, Dynamic Policy Programming (DPP) [4] and take the resultant path as the final output of the path planner. The motivation for this is

[1] J. Poon and J. Valls Miro are with the Faculty of Engineering and IT, University of Technology Sydney, Australia.

[2] Y. Cui, T. Matsubara and K. Sugimoto are with the Graduate School of Information Science, Nara Institute of Science and Technology, Japan.

that we believe expert demonstration must capture some of the expert's awareness of the PMD's geometric properties and what they consider to be desirable vehicle behavior, so it is much more beneficial for a framework to learn from and exploit this information for navigation purposes rather than having parameters tuned to suit different environments and platforms. A subsequent compliance model, also built from training data, then continually assesses the correlation between the path and the user's joystick input allows the planner to readily replan towards likelier intentions.

This combined intention estimation and path planning framework is then taken to areas unvisited in training data where it is assessed in novel and large environments without further calibration for new settings or users. Section IV assesses framework performance in novel settings with users of varying PMD proficiency. Sections V-VI discuss comparisons to other methodologies in assistive PMD navigation, the outcomes of this work and avenues for future work.

II. Local Intention Estimation

Most inferences on likeliest intention points defined solely within the PMD's immediate space should be as far from the PMD's origin as training data reasonably allows. This is primarily due to the platform's sheer footprint size; the unit in Fig. 1 measures approximately 0.8m from origin to front, and 0.7m across. For driving a PMD of this size its user needs to plan manoeuvres that consider a local space of several metres around to allow adequate room for delicate tasks such as aligning him/herself with a doorway, and it is reasonable to assume a planning algorithm would also benefit from a comparable area.

There is also an upper bound when planning paths for continuous navigation assistance. Excessive length is unnecessary as put forward by Huntemann et al. [5], as a path can be considered correct so long as it coincides with the user's desire for a brief interval. When constantly evaluating the fitness between the path being currently tracked by the PMD and the user's latent intention, there is no need to plan paths too far as the user can always indicate a change in intention. Hence the quantity of local space needed can be thought of as a soft region between the lower bound defined by the requisite space required for planning for a PMD of a given size, and the upper bound beyond which additional computation is mostly wasted.

As the DPP component in the subsequent path planner works in a grid-world scenario, we discretise the local space around the wheelchair and plan in a grid defined as a 5m square around the PMD with a cell resolution of 0.05m for an acceptable path planning time (<0.5s).

A. Intention Estimation Behavioral Modelling

Demonstration data contains expert actions $\mathbf{a}_{1:N}$ of 2D Cartesian joystick positions, odometry information $\mathbf{o}_{1:N}$ containing the platform's Cartesian position, heading and linear and angular velocities, and sensor data $\mathbf{z}_{1:N}$ consisting of a sweep of distances to obstacles across the on-board laser scanner's 180° horizontal field of view. This data is first

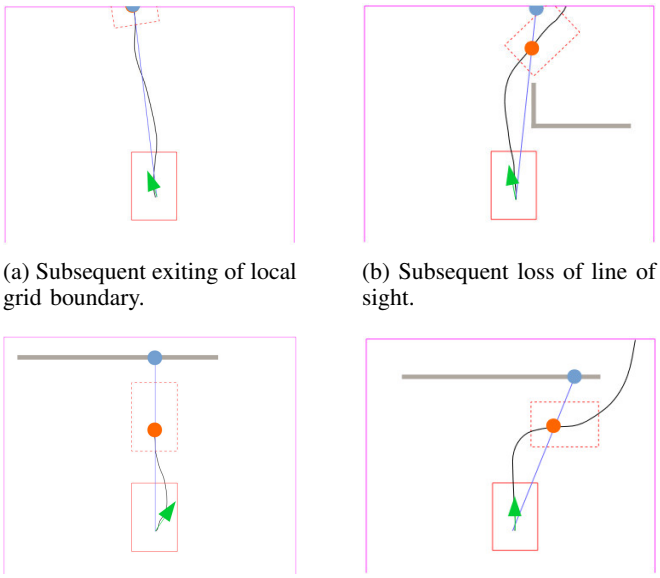

(a) Subsequent exiting of local grid boundary.

(b) Subsequent loss of line of sight.

(c) Inflection in vertical joystick axis.

(d) Orientation change of ≥ 90°.

Fig. 2: Conditions for extracting local paths with origin at the solid red PMD footprint, from a longer expert trajectory (black). Training data at the local termination point (orange point) is recorded, consisting of the expert joystick input at the origin, and the range of the beam (blue line capped with blue circle) from an on-board laser scanner that covers the termination point. Gray contours represent edges of obstacles perceived by the laser scanner, green arrows represent joystick position, and magenta lines represent the boundary of the PMD's local path-planning space.

decomposed into a series of short paths which terminate when any of the termination criteria in Fig. 2 are met. Given each local path (black line), a training data instance for the cell in which the path's terminal point lies (orange circle) is recorded. For a path starting at pose o_n, a training data instance consists of $\{a_n, r_\theta\} = 1$ where (r, θ) is the polar co-ordinate of the blue circle, representing the end point of the laser beam (blue line) nearest in angular orientation to the path's terminal point from laser scan sweep z_n. Beams reaching beyond the local grid (magenta lines) centred to o_n are capped at the grid border. Only edges of obstacles perceived in z_n are considered as we believe therein contains sufficient information for a human to also make an instantaneous decision. Paths are recorded from all training data instances $1, \ldots, N$.

This beam-style model is used in order to alleviate the effects of the curse of dimensionality when working with high dimensional laser scan data. Rather than attempting to match instances of $z_{1,\ldots,N}$ in their entirety to the new z^* as this would be easily overfitted, this approach allows for improved tolerance to large variation in environmental structure while retaining some information on the latent relationship between z and the sense of space the expert afforded the PMD.

Each grid cell containing training data then has its own

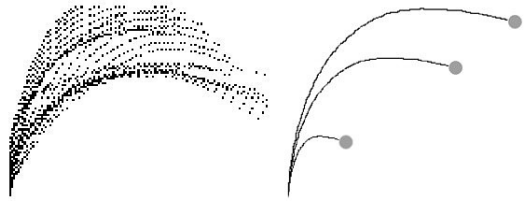

Fig. 3: Paths from training data sharing a similar endpoint orientation are gathered (left); their resulting primitive can then be spatially scaled to arbitrary poses (right, gray circles).

one-class classifier built as training data has only positive examples. Radial Basis Function Networks [6] are used for the intention likelihood estimate $P(y|a^*, r^*_\theta)$ of each cell for which data was present, given new joystick input a^* and range information r^*_θ. As $y = 1$ is a solution, a strong 0 prior is employed to reduce overfitting. Normalising p across the grid yields a discrete intention distribution, from which the center of the likeliest cell is taken as the intended goal point.

III. Local Path Planning

This section presents our local path planning method, and the control scheme for compliant path tracking. As the singular goal points from Sec. II-A do not provide information about the expert user's driving behavior, we aim to capture the expert's driving style in the form of primitive paths (Sec. III-A) that can be readily scaled to potential goal points. This expert-styled path, along with obstacles perceived by the on-board laser scanner is used to initialize a baseline reward function, allowing DPP (Sec. III-B) to compute an optimal grid-world traversal policy in the form of a Markov Decision Process.

The resultant path drawn from the final DPP policy (Sec. III-C) then becomes the path to be tracked. We use the same training data to formulate an inverse joystick model (Sec. III-D) to estimate the user's compliance to the current path given their input, allowing them to request a new path whenever the user changes his/her mind or the remainder of the current path proves to be incorrect.

A. Local Path Primitives

From the training data, local paths with similar endpoint orientations are gathered and a primitive is obtained as a least-squares solution after spatially scaling the paths to the same endpoint. In this work we use 17 discretized endpoint orientions for creating expert-styled path primitives. Then for a goal point (x,y) with a desired endpoint orientation of β, a path primitive with an endpoint orientation nearest to β is spatially scaled to reach it. Fig. 3 shows an example of a scaled primitive extracted from multiple expert paths. In this work the primitive starting with the nearest fit to the joystick orientation is taken.

B. Dynamic Policy Programming

Stochastic optimal control learns a Markov Decision Process (MDP) defined by a 5-tuple $(\mathcal{S}, \mathcal{A}, \mathcal{T}, \mathcal{R}, \gamma)$. $\mathcal{S}$ is a finite set of states, $\mathcal{A}$ is a finite set of actions, $\mathcal{T}^a_{ss'}$ is the transition probability from state s to state s' under the action a, $r^a_{ss'} = \mathcal{R}(s,s',a)$ is the reward from state s to state s' under the action a. Here we define $\mathcal{S}$ as a small grid-world around the PMD for planning paths in, with $\mathcal{A}$ consisting of 9 moves from a cell to one of its immediate neighbors or to itself. $\gamma \in (0,1)$ is the discount factor. The policy $\pi(a|s)$ denotes the probability of taking the action a under the state s. The value function $V_\pi(s) = \lim_{k\to\infty} \mathbb{E}_\pi\big[\sum_{k=1}^{K} \gamma^{k-1} r_{s_{t+k}} | s_t = s\big]$ is the expected return when the process starts in s and the decision maker follows the policy π. The solution of MDP is an optimal policy π^* that attains the maximum expected reward:

$$\pi^* = \arg\max_\pi \sum_{\substack{a\in\mathcal{A} \\ s'\in\mathcal{S}}} \pi(a|s)\mathcal{T}^a_{ss'}\big(r^a_{ss'} + \gamma V^*(s')\big), \forall s \in \mathcal{S}. \tag{1}$$

DPP builds a new value function by adding the Kullback-Leibler divergence to the reward function $\mathcal{R}$ as a penalty term. The Kullback-Leibler divergence between the policy π and the baseline policy $\bar{\pi}$ and the new value function V are defined as:

$$g^\pi_{\bar{\pi}}(s) = KL(\pi\|\bar{\pi}) = \sum_{a\in\mathcal{A}} \pi(a|s) \log\Big(\frac{\pi(a|s)}{\bar{\pi}(a|s)}\Big), \tag{2}$$

$$V_{\bar{\pi}}(s) \triangleq \lim_{k\to\infty} \mathbb{E}_\pi\Big[\sum_{k=1}^{K} \gamma^{k-1}\Big(r_{s_{t+k}} - \frac{1}{\eta} g^\pi_{\bar{\pi}}(s_{t+k-1})\Big)\Big| s_t = s\Big] \tag{3}$$

where $\mathbb{E}_\pi$ denotes expectation over transition model $\mathcal{T}$ and the current policy π. Parameter $\eta \in [0,1]$ is a constant that controls the Kullback-Leibler divergence term.

According to [4], the action preferences function [7] for all state action pairs $(s,a) \in \mathcal{S}\times\mathcal{A}$ in the k-th iteration are defined as $\Psi_k(s,a) = \frac{1}{\eta}\log\bar{\pi}^{k-1}(a|s) + \sum_{s'\in\mathcal{S}} \mathcal{T}^a_{ss'}\big(r^a_{ss'} + \gamma V^{k-1}_{\bar{\pi}}(s')\big)$. It represents the closed form of the optimal policy π^* following:

$$V^{k+1}_{\bar{\pi}}(s) = \frac{1}{\eta}\log\sum_{a\in\mathcal{A}} \exp(\eta\Psi_k(s,a)), \tag{4}$$

$$\bar{\pi}^{k+1}(a) = \frac{\exp\big(\eta\Psi_k(s,a)\big)}{\sum_{a'\in\mathcal{A}}\exp\big(\eta\Psi_k(s,a')\big)}. \tag{5}$$

The optimal action preferences function determines DPP's optimal policy according to Eq. 5. The update recursion of Ψ follows:

$$\Psi_{k+1}(s,a) = \Psi_k(s,a) - \mathcal{M}_\eta\Psi_k(s) + \sum_{s'\in\mathcal{S}} \mathcal{T}^a_{ss'}\big(r^a_{ss'} + \gamma\mathcal{M}_\eta\Psi_k(s')\big) \tag{6}$$

where $\mathcal{M}_\eta\Psi_k(s)$ is the the Boltzmann soft-max operator:

$$\mathcal{M}_\eta\Psi(s) = \sum_{a\in\mathcal{A}} \frac{\exp\big(\eta\Psi(s,a)\big)\Psi(s,a)}{\sum_{a'\in\mathcal{A}}\exp\big(\eta\Psi(s,a')\big)}. \tag{7}$$

Following Eq. 6, DPP updates action preferences function Ψ to iteratively optimize its value while upholding smoothness in its policy updates as determined by η.

C. Path Generator Using DDP

In order to use expert-styled paths with DPP, a baseline reward grid-world is set (Eq. 5). Cells along the scaled primitive receive increasingly positive reward, whereas obstacle cells from the laser scanner with 0.3m inflation receive a negative reward. DPP then optimizes its policy grid-world by smoothly updating with consideration to this baseline, and the resultant path drawn from the final policy is then followed.

Given initial action preferences $\Psi_0(\cdot,\cdot)$, DPP parameters γ, η and the number of iterations K, the process of the path generator is summarised in Algorithm 1.

Algorithm 1: Process of path generator using DPP

input : $\Psi_0(\cdot,\cdot)$, γ, η, K

/* DPP loop */

for $k = 1,2,3,...,K-1$ **do**

  for $(s,a) \in \mathcal{S} \times \mathcal{A}$ **do**

    calculate s', the next state of s under action a

    $\mathcal{T}_k\Psi_k(s,a) = r^a_{ss'} + \gamma\mathcal{M}_\eta\Psi_k(s')$

    $\Psi_{k+1}(s,a) = \Psi_k(s,a) + \mathcal{T}_k\Psi_k(s,a) - \mathcal{M}_\eta\Psi_k(s)$

/* generate path */

$i = 0$; $s_0 \leftarrow$ position of occupancy grid origin

while s_i *is within occupancy grid* **do**

  $a_i = \arg\max_{a\in\mathcal{A}} \Psi_{k+1}(s,a)$

  calculate s_{i+1}, the next state of s_i under action a_i

  $i = i+1$

output: assistance path $\{s_1, s_2, ..., s_{i-1}\}$

D. Path Compliance Model

Path tracking via the Pure Pursuit tracking algorithm [8] commences immediately once a path is acquired from DPP and transformed into global co-ordinates. The magnitude of the joystick's polar displacement scales the tracker's output linear and angular velocities, allowing the user to always control the rate of PMD motion. At each step the tracker provides an immediate control point on the path ahead of the PMD by a fixed distance, from which command velocities are derived. Since this point is always in the PMD's frame of reference it serves as a convenient focus to assess the user's desire to go to the control point, and arguably the remainder of the current generated path. A compliance model for potential control points around the PMD is built in a similar manner to the intention estimation sensor model however only the joystick input is considered, resulting in a compliance estimate $P(y|a^*)$. Either insufficient compliance or the control point nearing the end of the path results in a new intention and path computation.

IV. Experimental Results

Training data was obtained in a simulated house environment (20m x 10m) by an able user driving a PMD-like platform. The training paths followed by the user are shown in Fig. 4, who was tasked with driving throughout the space

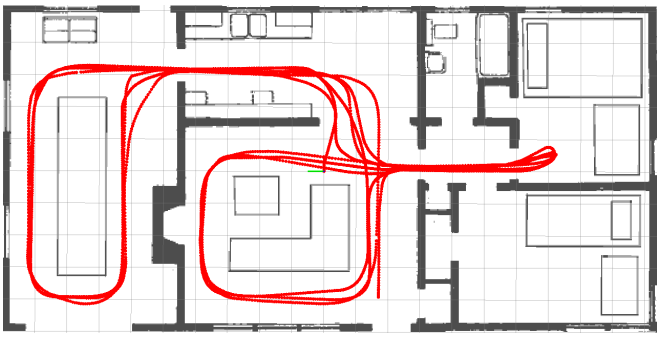

Fig. 4: Training data (red) from an able user in a 20m x 10m simulated home environment.

Fig. 5: Visualization of accuracy of the intention estimator and path generator, for a user mimicking the mean path (blue) of 5 other able users in a 7m x 5.5m simulated task. For more details please refer to the caption of Fig. 6, here the RMSE is 0.08m.

while maintaining safe distances to obstacles and walls. This could have also been done on the real platform, but we feel one of the advantages of the proposed framework is its ability to capture and generalise reasonable driving behaviors, so by simulating the dynamics and interactions it is shown how the process can be extended to different layouts, platforms and sensing characteristics, which can then be incorporated and tested on the real platform, as explained below (a scenario depicted by Fig. 6).

One the models were learned, the framework was first tested in a different indoor setting (7m x 5.5m) with the task of passing through a doorway and approaching a table (Fig. 5). This represents an environment deliberately laid out so that expected paths to be followed by a PMD user between a start and a goal point can be reasonably constrained. Given the challenge of accurately measuring an "intention", this exercise allows us to establish a metric of the performance of the intention estimation and path planning in generating paths that are close to what an expert would do. As expected, an able user performing the task unassisted produced paths in a manner comparable to the mean paths of 5 other unassisted

Fig. 6: Visualization of accuracy of the intention estimator and path generator, run *a-posteriori* for each of the logged points along an able user's free path (gray with PMD footprints). The first 50% of each generated path are shown here in green and red, with green representing points lying within 0.1m RMSE between generated path points and the user's path. Conducted on UTS campus in a space measuring approx. 60m x 27m on the UTS semi-autonomous wheelchair.

able users tasked to do the same, shown in blue in the Figure. The intention estimator and path generator were then run *a-posteriori* on each recorded point along their driven path. Here we consider the first 50% of each generated path for the metric of, upholding the notion that a path has to be 'correct' only for a reasonable portion of its length.The RMSE (root mean-square error) between the truncated estimated path points to the inferred intention point, and the effective user's driven path is 0.08m, showing a strong correlation between the proposed paths and what an able user deemed to be near-optimal navigational behavior in a novel exercise. For reference, points in red indicate estimated intended paths that lie beyond a 0.1m RMSE between the planned and actually executed path.

Similar evaluation of the intention estimation on the UTS semi-autonomous wheelchair (Fig. 1) is shown in Fig. 6. It can be seen how most of the initial 50% of the paths generated *a-priori* along the final paths traversed as estimated by the proposed navigational framework yielded an RMSE with 0.1m (shown in green), showing the system's ability to generalize to large open areas despite being trained in a restrictive house-like indoor space. PMD localization and map building was handled by Hector SLAM [9].

To assess the framework's overall ability to provide assistance to less capable users, an 82 year old female volunteer with deficiencies typical of her age and without prior PMD experience was first requested to attempt the same task of doorway navigation and table approach (Fig. 7a). A collision occurred while attempting to pass through the doorway which required a small reversal to fix, and pulling over at the table involved turning in place before a final straight approach. Fig. 7b shows the same task undertaken with the assistive framework in operation. The framework was capable of providing generated paths across the entire duration of travel, with a more gradual approach to the final destination resulting in minimal turning in place for aligning with the table edge. The path travelled with the aid of the assistive framework is noticeably smoother and devoid of collisions, and ends with the PMD reaching the table while being closer to the wall to the right of its final pose. For further testing, 5 able users subject to Gaussian noise of $\mathcal{N}(0, 0.3)$ on the joystick ($\in (-1, 1)$) were requested to attempt the task (Fig. 8). All 5 were able to pass through the doorway, although some difficulties were encountered in terms of aligning with the table. $95 \pm 7\%$ of all points fit within the 2σ bound from paths by the same 5 users without assistance or input signal interference, indicating a degree of robustness against user tremoring.

Experimentation was conducted on an i7 Linux machine with 16 GB RAM and Nvidia 980M GPU. An average intention inference and path generation cycle took $<$0.5s in addition to minor latencies arising from MATLAB/ROS (`www.ros.org`) communications.

V. Related work and discussion

A. Intention Estimation for PMDs

Conventional active navigational assistance with PMDs tend to rely on *a-priori* map building of the entire space that the system is expected to operate in. Selected locations of interest in this space correspond to destinations that can be perceived as longer-term targets. Examples include key points in a home allowing easy access to furniture

or household utilities, or strategically placed in especially difficult areas such as doorways that require intervention for safe traversal [10]. For an intelligent system to provide timely assistance while manoeuvring, the tendency is to evaluate the most likely intended target with some form of classification, postulated on prior learnings from demonstrative navigational data typically gathered from end-users or able-bodied demonstrators. This long-term destination likelihood classification has already been previously addressed by several inference methodologies including Dynamic Bayesian Networks [11], Heirarchical Hidden Markov Models [12], Gaussian Processes [13], Artificial Neural Networks [14] as well as heuristic multi-hypothesis consideration [15].

The critical shortcoming of approaches reliant on known environments is the requirement of maintaining considerable spatial maps to accomodate longer-term assistive planning, and the computational complexity associated to that. Moreover, preserving inference accuracy over time in deployment scenarios where both environmental configuration and user preferences change, such as in a shopping center or the local neighbourhood, requires significant upkeep. It is effectively infeasible to attempt to map and provide targets for all the places a PMD user would go in everyday life for any sizeable environment. Instead this paper describes an approach to build probabilistic models for local intention estimation within a moving window aroud the user, allowing for a system to provide intention estimates and navigational assistance "anywhere". Circumventing the curse of dimensionality from high-dimensional laser scan data by considering a beam-type sensor model for intention estimation makes this methodology, to the best of our knowledge, the first to perform local intention estimation as per demonstration data.

B. Assisted Navigation and Path Planning

Local assistive navigation for PMDs is rather well established, with possibly the simplest being systems such as the Bremen Autonomous Wheelchair [16] that nullify inputs which would result in collision. Obstacle avoidance algorithms are frequently used, for instance the Vector Field Histogram [17] on the NavChair [18] platform or protocols tailored to specific sensor arrangements [19]. This approach still requires some rudimentary intention estimation to occasionally override pure obstacle avoidance protocols as near-collisions have to occur to allow for actions like parking close by furniture.

Fusion of robot command signals with that from the user is a common approach for shared autonomy [20]–[22], employing a metric of 'goodness' on the part of the user to dictate their share of a final control signal composed of a weighted sum. These metrics are usually defined as a combination of heuristic measurements including proximity to obstacles and the smoothness of user input. However we believe it is inherently safer for the user to provide suggestions to a system fully in control of platform behavior rather than to share control in this manner, as there is little guarantee the combined control signal is safe or desirable even if the individual signals comprising it are.

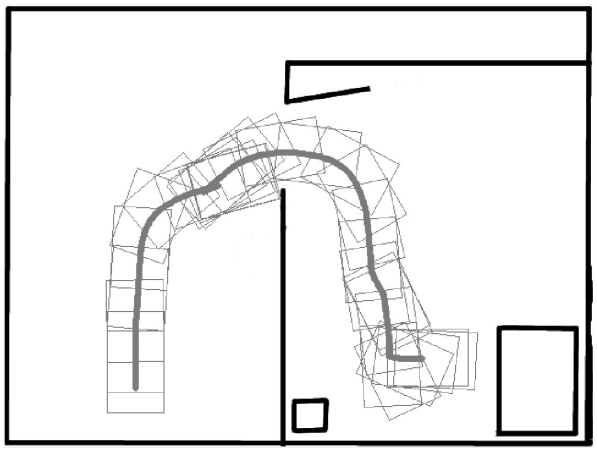

(a) Unassisted path.

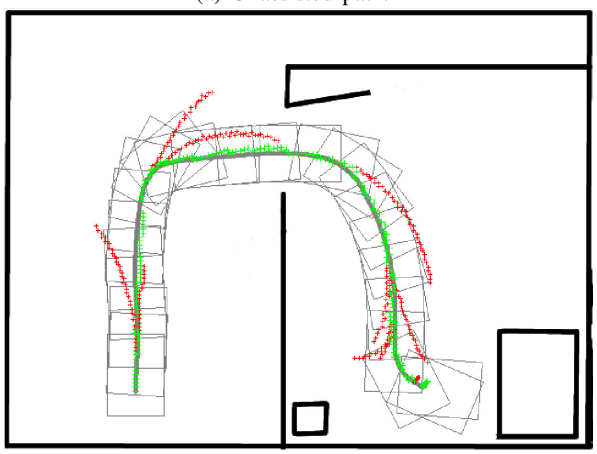

(b) Assisted path (gray) with compliant generated path points (green) and incompliant (red).

Fig. 7: Comparison between unassisted and assisted paths taken by an 82 year old female volunteer.

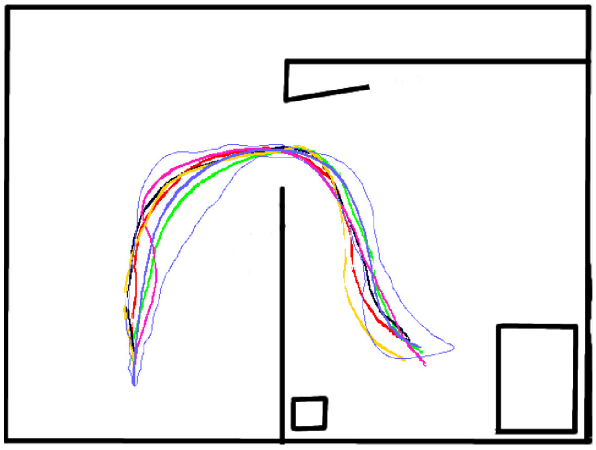

Fig. 8: Assisted paths of 5 able users with joystick input subject to $\mathcal{N}(0, 0.3)$ Gaussian noise, over μ and 2σ of unassisted and unhindered paths by the same users (blue).

It bears noting that the most common approach for mobile robot path planning still largely remains in the domain of optimizing over a gridworld due to their versatility and lower computational cost, so it is the method we have also incorporated for this work. The reduced proximity of our intentions allows us to define a spatially adaptable set of curves extracted from training data which can then be concatenated along the PMD's journey, in a manner similar to the chaining of Dynamic Movement Primitives [23] in the Hybrid A* algorithm [24].

VI. Conclusions

In this paper a framework for PMD assistance is proposed, capable of inferring short-term destinations and their subsequent navigation. A probabilistic sensor model only reliant upon immediately available user input data and laser range information is built from demonstration driving data from an able expert to provide estimates of the most likely point a user wishes to pass through or stop at in a given instant. The same training data set is then also used to regress path primitives and an inverse joystick model to assess compliance with the user. Path primitives extracted from training data and spatially scaled to these intentions are subsequently refined via Dynamic Policy Programming, a stochastic optimization process smoothly combining sensor data with movements along the provided baseline path.

Validation of the intention estimation and path planning engine revealed a 0.08m RMSE between the first 50% of paths generated *a-posteriori* and an able user in a novel setting. Similar evaluation with a real wheelchair in an open lobby environment on UTS campus yielded an RMSE below 0.1m, indicating the intention estimator's ability to generalize to differing environments. An 82-year old volunteer with no prior experience of PMD use was able to complete a complex task of driving through a doorway and approaching a table, without the collisions and awkward manoeuvres present in an attempt without assistance.

Future work will focus on the use of a continuous probabilistic framework to better capture intention distributions across the local space, as well as an improved methodology for base path selection or generation.

Acknowledgements

This work was supported by the 2015-2017 JSPS Bilateral Joint Research Projects (Open Partnership) for collaboration between NAIST and UTS. We also wish to express our gratitude to all who participated in the experiments.

References

[1] United Nations, "United nations 2006 world populations prospects: The 2006 revision," tech. rep., United Nations, New York, 2006.

[2] Tegart, "Smart technology for healthy ageing," tech. rep., ATSE, 2010.

[3] "Mass 24 - home access checklist - power-drive wheelchairs (pwc)." `https://www.health.qld.gov.au/mass/documents/form-mass24-home-access-safety.pdf`. Accessed: 2016-09-12.

[4] M. G. Azar, V. Gómez, and H. J. Kappen, "Dynamic policy programming," *The Journal of Machine Learning Research*, vol. 13, no. 1, pp. 3207–3245, 2012.

[5] A. Huntemann, E. Demeester, G. Vanacker, D. Vanhooydonck, J. Philips, H. V. Brussel, and M. Nuttin, "Bayesian plan recognition and shared control under uncertainty: assisting wheelchair drivers by tracking fine motion paths," in *2007 IEEE/RSJ International Conference on Intelligent Robots and Systems*, pp. 3360–3366, 2007.

[6] M. Orr, "Introduction to radial basis function networks," tech. rep., University of Edinburgh, Scotland, 1996.

[7] R. S. Sutton and A. G. Barto, *Reinforcement learning: An introduction*. MIT press Cambridge, 1998.

[8] R. Coulter, "Implementation of the pure pursuit path tracking algorithm," tech. rep., Carnegie Mellon University, Pittsburgh, 1990.

[9] S. Kohlbrecher, J. Meyer, O. V. Stryk, and U. Klingauf, "A flexible and scalable slam system with full 3d motion estimation," in *Proc. IEEE International Symposium on Safety, Security and Rescue Robotics (SSRR)*, IEEE, November 2011.

[10] M. Derry and B. Argall, "Automated doorway detection for assistive shared-control wheelchairs," in *Robotics and Automation (ICRA), 2013 IEEE International Conference on*, pp. 1254–1259, May 2013.

[11] A. Huntemann, E. Demeester, E. Poorten, H. Van Brussel, and J. De Schutter, "Probabilistic approach to recognize local navigation plans by fusing past driving information with a personalized user model," in *Robotics and Automation (ICRA), 2013 IEEE International Conference on*, pp. 4376–4383, May 2013.

[12] M. Patel, J. V. Miro, and G. Dissanayake, "A probabilistic approach to learn activities of daily living of a mobility aid device user," in *Proceedings of the IEEE International Conference on Robotics and Automation, ICRA Hong Kong, China*, pp. 969–974, 2014.

[13] T. Matsubara, J. Miro, D. Tanaka, J. Poon, and K. Sugimoto, "Sequential intention estimation of a mobility aid user for intelligent navigational assistance," in *Robot and Human Interactive Communication (RO-MAN), 2015 24th IEEE International Symposium on*, pp. 444–449, Aug 2015.

[14] J. Poon, J. V. Miro, and R. Black, "A passive estimator of functional degradation in power mobility device users," in *2015 IEEE International Conference on Rehabilitation Robotics (ICORR)*, pp. 997–1002, Aug 2015.

[15] T. Carlson and Y. Demiris, "Human-wheelchair collaboration through prediction of intention and adaptive assistance," in *Robotics and Automation, 2008. ICRA 2008. IEEE International Conference on*, pp. 3926–3931, May 2008.

[16] A. Lankenau, O. Meyer, and B. Krieg-Bruckner, "Safety in robotics: the bremen autonomous wheelchair," in *Advanced Motion Control, 1998. AMC '98-Coimbra., 1998 5th International Workshop on*, pp. 524–529, Jun 1998.

[17] J. Borenstein and Y. Koren, "The vector field histogram-fast obstacle avoidance for mobile robots," *IEEE Transactions on Robotics and Automation*, vol. 7, pp. 278–288, Jun 1991.

[18] R. C. Simpson and S. P. Levine, "Automatic adaptation in the navchair assistive wheelchair navigation system," *IEEE Transactions on Rehabilitation Engineering*, vol. 7, pp. 452–463, Dec 1999.

[19] H. Kitagawa, T. Kobayashi, T. Beppu, and K. Terashima, "Semi-autonomous obstacle avoidance of omnidirectional wheelchair by joystick impedance control," in *Intelligent Robots and Systems, 2001. Proceedings. 2001 IEEE/RSJ International Conference on*, vol. 4, pp. 2148–2153, 2001.

[20] Q. Li, W. Chen, and J. Wang, "Dynamic shared control for human-wheelchair cooperation," in *Robotics and Automation (ICRA), 2011 IEEE International Conference on*, pp. 4278–4283, May 2011.

[21] C. Urdiales, J. M. Peula, M. Fdez-Carmona, C. Barrué, E. J. Pérez, I. Sánchez-Tato, J. C. del Toro, F. Galluppi, U. Cortés, R. Annichiaricco, C. Caltagirone, and F. Sandoval, "A new multi-criteria optimization strategy for shared control inwheelchair assisted navigation," *Autonomous Robots*, vol. 30, no. 2, pp. 179–197, 2011.

[22] A. Goil, M. Derry, and B. D. Argall, "Using machine learning to blend human and robot controls for assisted wheelchair navigation," in *Rehabilitation Robotics (ICORR), 2013 IEEE International Conference on*, pp. 1–6, June 2013.

[23] S. Schaal, "Dynamic movement primitives - a framework for motor control in humans and humanoid robotics," *Adaptive Motion of Animals and Machines*, pp. 261–280, 2006.

[24] D. Dolgov, S. Thrun, M. Montemerlo, and J. Diebel, "Path planning for autonomous vehicles in unknown semi-structured environments," *The International Journal of Robotics Research*, vol. 29, no. 5, pp. 485–501, 2010.